JOURNAL OF MATERIALS SCIENCE 20 (1985) 1061–1068

On the mechanism of facetted growth

ROGER WEST, HASSE FREDRIKSSON
Department of Casting of Metals, Royal Institute of Technology, S-10044 Stockholm, Sweden

The morphology of silicon crystal precipitate in a hypereutectic Al–Si alloys is analysed. The morphology is investigated at different cooling rates. A theoretical model describing the growth of facetted crystals is developed. The most important parameters for the formation of the observed crystals are determined.

1. Introduction

Many different morphologies have been observed on crystals grown from melt and vapour. The most common types of crystals formed from a melt are the dendrite (composed of rounded branches), and the facetted crystal, which can be cubic, octahedral, columnar or platelike. A transition between the dendritic and facetted form is also observed. In this paper a simple mathematical model for the crystal growth is derived. It takes into account anisotropy in the surface tension as well as the interfacial reaction, and it also explains the formation of facetted crystals. Silicon crystals precipitated in hypereutectic aluminium–silicon alloys are discussed first. The crystal morphology in this system varies with the cooling rate, nucleation frequency and small additions of alkaline metals such as sodium. Silicon crystals have a cubic lattice and the same crystal morphologies as many other metallic systems with the cubic lattice. The morphology was analysed with the help of the scanning electron microscope (SEM) in deep-etched samples.

2. Preparation of the samples

The same method as in the previous study [1] was used in this work. The alloy with 17% silicon was made in a graphite mould with a diameter of 50 mm. From this alloy samples of 15 g were taken and treated with sodium. The samples were solidified by moving them to the colder part of the furnace. The first experiment was made with sodium; in the second experiment the samples were held in the furnace for such a long time that most of the sodium was evaporated. The samples were then solidified. Small samples were taken for metallographic investigation. Preparation of the samples for SEM observations is described in our earlier paper [1].

3. Growth morphologies

Owing to twin planes in the crystals, various types of morphologies were observed in each sample. These forms were discussed in the earlier work. The present discussion only concerns crystals without twin planes.

3.1. Ingots

All the crystals observed in the ingot were formed with (1 1 1) facets. The ideal shape is octahedral. Fig. 1 shows an example of a nearly perfect crystal. Fig. 2 shows an example where the crystal has deviated from the ideal morphology. In this case the (1 1 1) facets contain holes and the corners have been elongated.

3.2. Sample with high sodium content

The effect of sodium is illustrated in Fig. 3. It shows that the crystals are now formed with (1 1 1) and (1 0 0) facets. The (1 0 0) facets are the dominant.

3.3. Sample with low sodium content

Figs. 4 and 5 illustrate the crystal morphologies observed in an alloy with low sodium content after slow solidification. The crystals are bounded by (1 1 1) and (1 0 0) facets.

4. Discussion

All of the crystals discussed may be characterized as facetted. The facet is often explained as an effect of anisotropic growth where the most slow-

0022–2461/85 $03.00 + .12

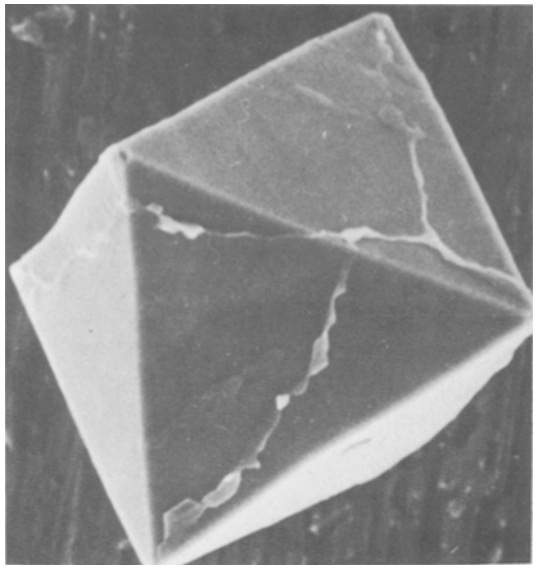

Figure 1 The octahedral shape of one silicon crystal.

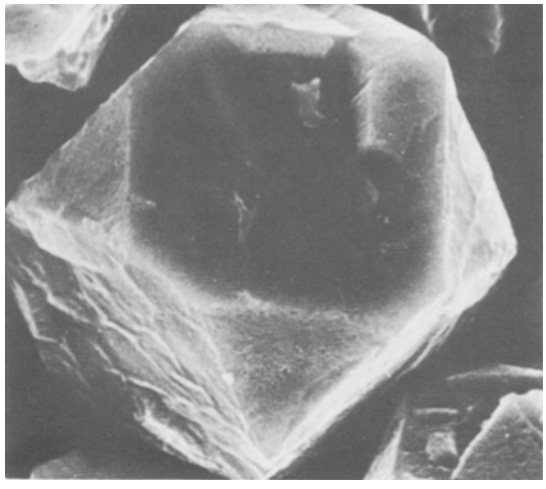

Figure 3 Facetted silicon crystal with both [100] and [111] facets. High sodium content.

growing facet becomes dominant. This is true if the growth is not limited by the rate of transport of matter or heat in the surrounding matrix. In order to analyse the growth process in detail, one has to consider both the interface reaction and the diffusion process outside the growing crystal. In addition, one has to consider the effect of surface tension on the growth rate. An isotropy of the surface tension might influence the shape of the crystal. These three variables influence the crystal morphology during solidification. The diffusion field around a growing facetted crystal was experimentally studied by Berg [2] and Humphreys-Owen [3]. For relatively small crystals, Humphreys-Owen found that the diffusion field around a growing crystal was nearly spherical. Fig. 6 shows an example. The lines around the crystal are isoconcentration lines. It is interesting to note that the concentration from the midpoint of a facet to the centre varies. This variation is described schematically in Fig. 7. The figure shows that the driving force for diffusion is largest at the midpoint and lowest at the corner. The supersaturation on the surface which is equal to the driving force for the interface reaction is smallest at the midpoint and largest at the corner.

This conclusion is now used in a comparison of the growth rates for two different facets. In order to examine the net effect of the mass transport and the interface kinetics, a treatment based upon the theory of diffusional growth of a spherical particle is used.

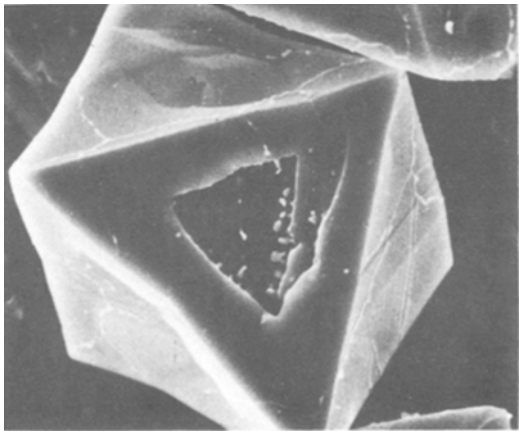

Figure 2 The start of the formation of a hopper crystal.

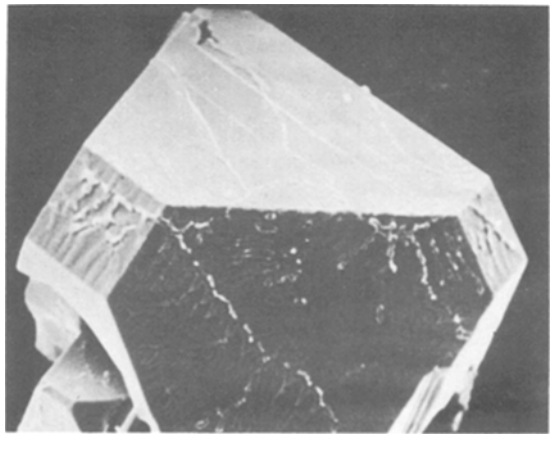

Figure 4 Facetted silicon crystals with both [100] and [111] facets. Low sodium content.

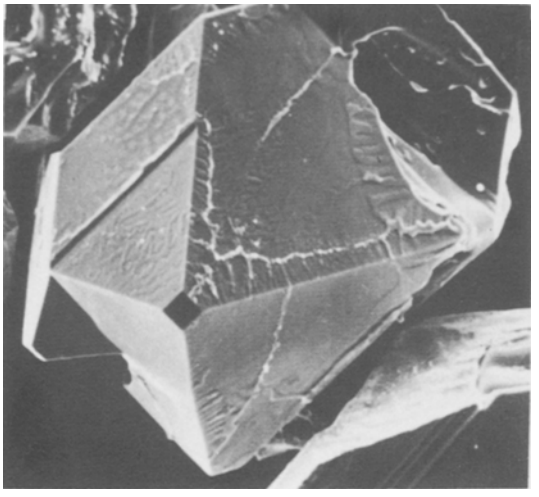

Figure 5 Same sample as in Fig. 4, illustrating that the facets can vary in size.

The shape of the particle is estimated by calculating the rate of the interface reaction in the diffusion field. In this work the effect of the surface tension on the growth process is also considered. The analysis starts with a derivation of the critical size of a facetted nuclei, which is to be used later in the growth theory.

4.1. The nucleation of facetted crystals

The classical method to determine the size of a nucleus is to consider the difference in free energy between a solid nucleus and the melt:

$$\Delta G_{\text{total}} = \frac{\Delta G_{\text{m}}}{V_{\text{m}}} V + \Sigma \sigma_{[\text{xxx}]} A, \qquad (1)$$

where ΔG_{m} is the difference in molar free energy between solid and melt, σ_{xxx} the specific surface free energy of facet, A the total area of facets (xxx), V_{m} the molar volume, and V the volume of particle. This equation is used to determine the critical size of the nucleus. In a system where the surface free energy is isotropic, the nucleus is a sphere with a critical size of:

$$R^* = \frac{2\sigma V_{\text{m}}}{(-\Delta G_{\text{m}})}. \qquad (2)$$

Normally the surface free energy is not isotropic. In this case the nucleus is dominated by the surfaces with the lowest free energies. For cubic systems, these surfaces are the (100) and (111) facets. In this treatment, only these two facets are considered. It is assumed that the surface free energies for all other facets are much larger. By minimizing the total surface free energy one obtains the shape of the crystal for a given volume. The distances from the centre of the crystal to the midpoint of a facet is given by the following expression.

$$R^*_{(111)} = \frac{2\sigma_{[111]} V_{\text{m}}}{(-\Delta G_{\text{m}})} \qquad (3)$$

$$R^*_{(100)} = \frac{2\sigma_{[100]} V_{\text{m}}}{(-\Delta G_{\text{m}})}. \qquad (4)$$

Equations 3 and 4 show that an octahedral is formed when σ_{100} is at least three times larger than σ_{111}. In the same way, σ_{111} must be three times larger than σ_{100} for a cubic nucleus. When the ratio σ_{100} for a cubic nucleus. When the ratio $\sigma_{100}/\sigma_{100}$ falls between $1/3^{1/2}$ and $3^{1/2}$ the nucleus will be bounded both by (100) and (111) facets.

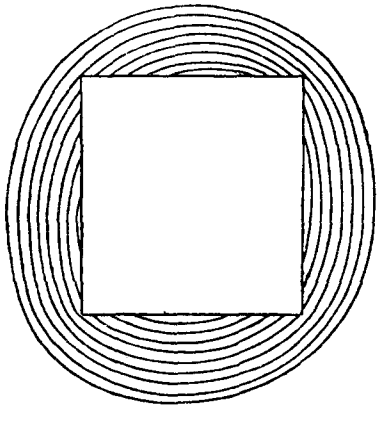

Figure 6 Isoconcentration lines around a growing facetted crystal according to Humphreys-Owen [3].

4.2. Spherical growth

The growth of a spherical particle in a dilute solution has been treated by several authors, e.g. Zener [4]. It has been shown that the concentration field can adequately be described by Laplace's equation:

$$X^{\text{L}} = A + \frac{B}{r} \qquad (5)$$

where r is the distance from the centre of the particle, and X^{L} the concentration in the liquid. By applying the proper boundary conditions, constants A and B can be determined.

$$X^{\text{L}} = X_0^{\text{L}} + \frac{X^{\text{L}/\alpha} - X_0^{\text{L}}}{r} R, \qquad (6)$$

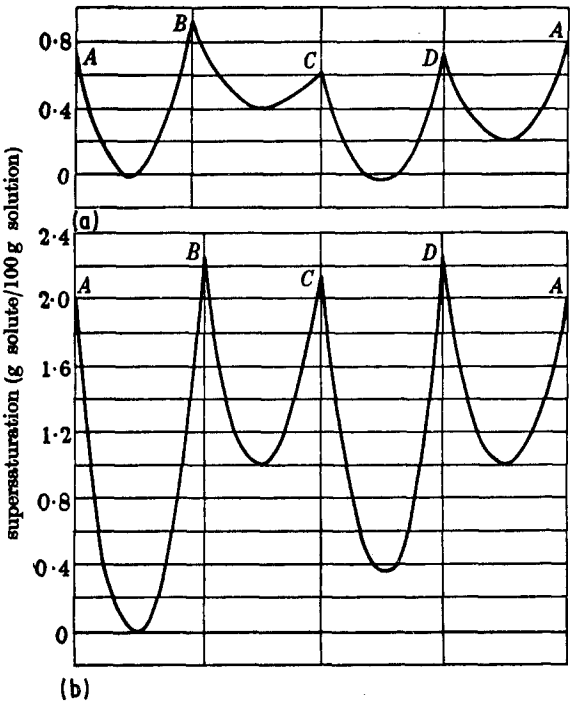

Figure 7 The concentration distribution at the surfaces of cubic crystals. The full vertical lines represent the corners of the crystal. From Humphreys-Owen [3].

where X_0^L is the initial composition and $X^{L/\alpha}$ is the composition of L in contact with the growing phase. R is the radius of the α-particle. The growth rate is estimated by using Fick's first law.

$$\frac{dR}{dt} = -D\left(\frac{dx}{dr}\right)_R / (X^{L/\alpha} - X^{\alpha/L}) = \frac{D}{R}\frac{X^{L/\alpha} - X_0^L}{X^{L/\alpha} - X^{\alpha/L}} \quad (7)$$

It was pointed out by Zener [5] that this expression shows that the growth rate tends to infinity when the radius tends to zero. This is impossible owing to the fact that the growth rate of a nucleus is zero. The normal way to treat this problem is to take into account that the driving force for diffusion decreases owing to the surface tension on the particle. According to Zener [5], this term can be related to the critical size for nucleation by the following relation:

$$X^{L/\alpha} - X_\sigma^{L/\alpha} = (X^{L/\alpha} - X_0^{L/\alpha})\frac{R^*}{R}. \quad (8)$$

The driving force can now be divided into two terms:

$$X^{L/\alpha} - X_0^L = (X^{L/\alpha} - X_\sigma^{L/\alpha}) + (X_\sigma^{L/\alpha} - X_0^{L/\alpha}). \quad (9)$$

The first term on the right-hand side describes the driving force necessary to form new surfaces. The second term on the right-hand side describes the driving force for the diffusion process and is given by Equation 7. Combining Equations 7, 8 and 9 gives:

$$\frac{dR}{dt} = \frac{D}{R} = \frac{(X^{L/\alpha} - X_0^L)[1 - (R^*/R)]}{(X^{L/\alpha} - X^{\alpha/L})}. \quad (10)$$

This equation describes the growth rate of a spherical particle influenced by surface tension.

4.3. The effect of interface kinetics

Equation 10 describes rather well the growth process when it is controlled by diffusion. When the interface reaction is slow it affects concentration at the interface and the growth rate as well. A simple way of combining the effect of diffusion, surface tension and interface kinetics is to divide the driving force into three terms:

$$X^{L/\alpha} - X_0^L = (X^{L/\alpha} - X_\sigma^{L/\alpha}) + (X_\sigma^{L/\alpha} - X_i^{L/\alpha}) + (X_i^{L/\alpha} - X_0^L). \quad (11)$$

The first term on the right-hand side gives the driving force due to the surface tension and is described by Equation 8. The second term gives the driving force for the interface reaction, and the last gives the driving force for the diffusion process. This term is identified as $X^{L/\alpha} - X_0^L$ in

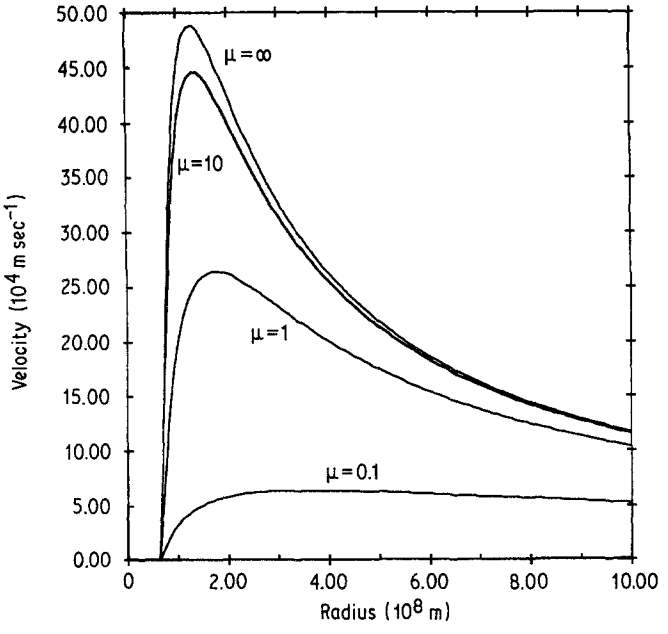

Figure 8 The growth velocity of a spherical particle as a function of particle size.

Equation 7. It may be complicated to describe the interface kinetics. It is often approximated by the following simple relation [6]:

$$\frac{dR}{dt} = \mu(X_\sigma^{L/\alpha} - X_i^{L/\alpha})^n, \qquad (12)$$

where μ and n are two constants. On the basis of theoretical modelling, n is often put equal to 1 or 2 but can have any value in between. In the present work n is assumed to be equal to 1. Inserting Equations 7, 8 and 12 into Equation 11 gives:

$$X^{L/\alpha} - X_0^L = (X^{L/\alpha} - X_0^L)\frac{R^*}{R} + \left(\frac{dR}{dt}\frac{1}{\mu}\right) + \frac{dR}{dt}\frac{R}{D}(X^{L/\alpha} - X^{\alpha/L}). \qquad (13)$$

This expression can be solved for constant values of $(X^{L/\alpha} - X_0^L)$ and $(X^{L/\alpha} - X^{\alpha/L})$. The growth rate as function of size is then described. By rearranging Equation 13 one obtains:

$$\frac{dR}{dt} = \frac{(X^{L/\alpha} - X_0^L)[1 - (R^*/R)]}{(R/D)(X^{L/\alpha} - X^{\alpha/L}) + (1/\mu)}. \qquad (14)$$

Calculations of the growth rate were performed with $D = 10^{-8}$ m^2 sec^{-1}, $X^{L/\alpha} - X^{\alpha/L} = 0.8$, $X^{L/\alpha} - X_0^L = 0.01$ and $\sigma = 0.1$ J m^{-2}.

Fig. 8 shows the results of the calculations and demonstrates the effect of different values of μ on the growth rate as function of particle size. The figure shows that the maximum growth rate occurs at larger values of R with decreasing μ. In order to analyse this in more detail, Equation 12 was derived and R for maximum growth rate is:

$$R_{max} = R^* + \left\{R^*\left[R^* + \frac{D}{\mu(X^{L/\alpha} - X^{\alpha/L})}\right]\right\}^{1/2}. \qquad (15)$$

It shows that in the limit $\mu \to \infty$, $R = 2R^*$. Fig. 9 shows R_{max} as a function of $D/[\mu(X^{L/\alpha} - X^{\alpha/L})]$. The figure shows that R_{max} is much larger than twice R^* for larger values of $D/[\mu(X^{L/\alpha} - X^{\alpha/L})]$. To find out the size of the particle as a function of time, Equation 14 was integrated from $t = 0$ to $t = t$ and $R = R_0$ to R. The integration gives:

$$t = \frac{1}{\mu(X^{L/\alpha} - X_0^L)}\left[R - R_0 + R^* \ln\left(\frac{R - R^*}{R_0 - R^*}\right)\right] + \frac{X^{L/\alpha} - X^{\alpha/L}}{D(X^{L/\alpha} - X_0^L)}\left\{\tfrac{1}{2}[(R - R^*)^2 - (R_0 - R^*)^2] + 2R^*(R - R_0) + R^{*2}\ln\left(\frac{R - R^*}{R_0 - R^*}\right)\right\}. \qquad (16)$$

Fig. 10 shows the size of the crystal as a function of time for different kinetic coefficients. All other values were the same as those used for calculation of Fig. 8.

4.4. Anisotropic growth

It was pointed out earlier that a facetted crystal is bounded by the slowest growing facets. If the

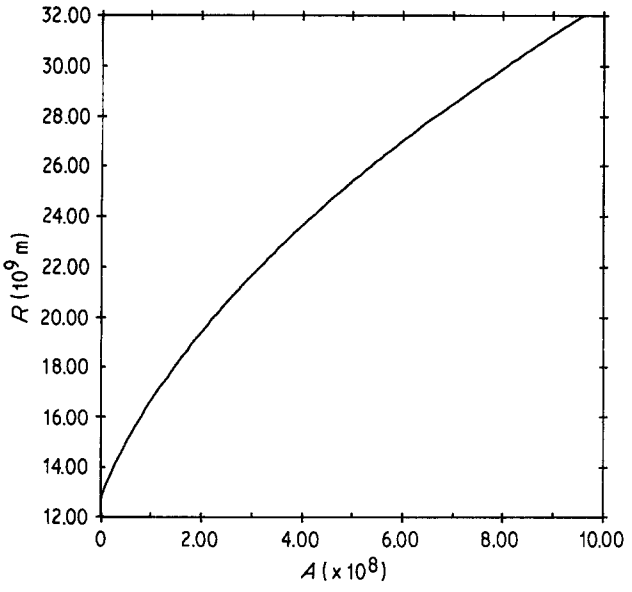

Figure 9 R_{max} as a function of $D/\mu(X^{L/\alpha} - X^{\alpha/L}) = A$. R^* is given in Fig. 8.

growth process is completely interface-controlled, Equation 12 describes the size and the shape of a crystal. The growth process is controlled by the diffusion process and the effect of the surface tension as well. It is difficult to make a theoretical analysis of the diffusion field around a facetted crystal. Using Equation 5 and interpreting R as the distance of the midpoint of the facet to the centre of the crystal and X^L as the composition of the liquid at the midpoint, denoted by R_{xxx} and $X^{L/\alpha}_{xxx}$ gives:

$$X^L = X^L_0 + (X^{L/\alpha}_{xxx} - X^L_0)R_{xxx}/r . \quad (17)$$

Corresponding to Equation 7, the advancement of the midpoint is described by:

$$\frac{dR_{xxx}}{dt} = \frac{D}{R_{xxx}} \frac{X^{L/\alpha}_{xxx} - X^L_0}{X^{L/\alpha}_{xxx} - X^{\alpha/L}} . \quad (18)$$

Equations 13 and 16 can be used to describe the growth rate of the midpoint of each facet, and also the distance from the centre of the crystal to the midpoint of a facet. The critical radius, R^*_{xxx}, is given by the nucleation theory. In view of the approximation of the concentration field it seems justified to use the further approximation that the facets are perfectly planar. Equation 16 can then be used to evaluate the relative size of different facets. For a cubic crystal we shall now only

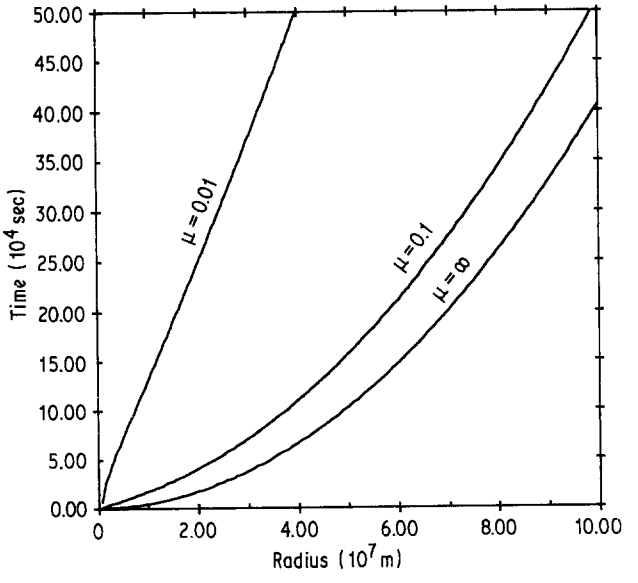

Figure 10 The size of a particle as a function of time; R^* is given in Fig. 8.

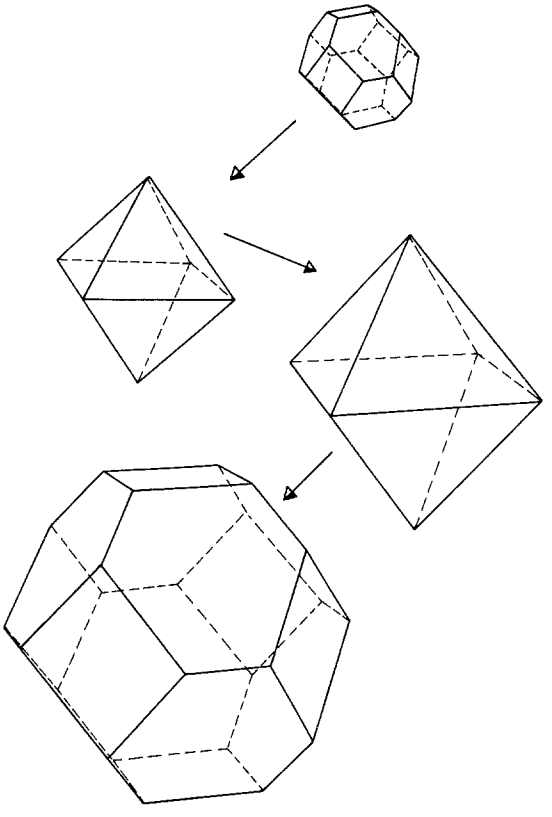

Figure 11 The change of crystal shape with increasing size.

consider the (100) and (111) facets. Fig. 11 illustrates a series of calculations giving the shape of the crystal as a function of time. In the calculations it is assumed that $\sigma_{100} = \sigma_{111}$, $\mu_{111} < \mu_{100}$.

The calculations show that the crystal from the beginning is an octahedral with cut off corners. Later on, owing to the anisotropy in the interface reaction, an octahedron is formed. When the size of the crystal increases, the shape will change and an octahedron with cut off corners forms again. This is due to the transport of matter being more important the larger the crystal is. In order to find out how the shape of a crystal is changed with different parameters, a series of calculations was performed to illustrate the formation of an octahedron. By using Equation 14 in the (100) and (111) directions, R_{111} and R_{100} as a function of t are calculated. In this calculation the ratio of μ_{111}/μ_{100} was varied and different values of A were used, where A is defined as:

$$A = R^*_{111}\mu_{111}\,(X^{L/\alpha} - X^{\alpha/L})/D\,.$$

Fig. 12 shows the results of the calculations. At values of A larger than 0.5 no octahedrons can form. Decreasing A gives a higher tendency for formation of octahedrons.

Fig. 11 indicates that the octahedron cannot preserve its shape when the size of the crystal is increasing. This effect is also illustrated in Fig. 12. At very low values of A the octahedral shape will persist until the crystal has reached a very large size. In this case the assumption of a spherical diffusion field does not hold. The corner will now grow faster than the sides and crystals such as the one illustrated in Fig. 2 will form and our simple model is no longer valid.

In our calculations, we have only treated a cubic system and only analysed growth in two different directions. It is possible to treat the

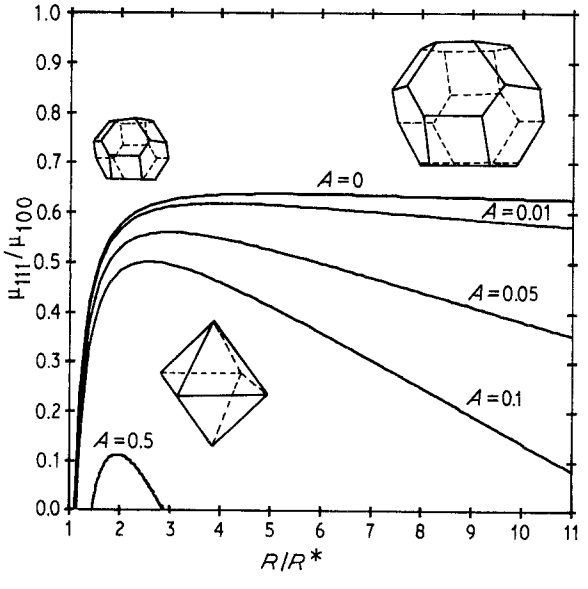

Figure 12 The change of crystal shape as a function of μ_{111}/μ_{100} for different values of $A = [R^*_{111}\mu_{111}(X^{L/\alpha} - X^{\alpha/L})]/D$.

growth in any direction and for the case of a smoothly varying kinetic coefficient, rounded crystals will form.

5. Conclusion

In this paper a simple theoretical model describes the formation of facetted crystals in melts. In spite of its simplicity the most important parameters for the formation of facetted crystals are analysed. The most dominant parameters are the interface kinetic and the transport of matter. The surface tension is effective only for very small crystals.

Acknowledgement

Many stimulating discussions with Professor Mats Hillert are acknowledged.

References

1. H. F. FREDRIKSSON, M. HILLERT and N. LANGE, *J. Inst. Metals* **101** (1973) 285.
2. W. F. BERG, *Proc. Roy. Soc.* **164A** (1938) 79.
3. S. P. F. HUMPHREYS-OWEN, *ibid.* **197A** (1949) 218.
4. C. ZENER, *J. Appl. Phys.* **20** (1949) 950.
5. *idem, Trans. AIME* **167** (1946) 550.
6. W. A. TILLER, "The Art and Science of growing crystals", edited by J. J. Gilman (Wiley, 1963).

Received 18 December 1983
and accepted 10 April 1984